Chalcogenide Letters Vol. 13, No. 1, January 2016, p. 27 - 34

HYDROTHERMAL SYNTHESIS AND CHARACTERIZATION OF ULTRATHIN MoS_2 NANOSHEETS

X.H. ZHANG[a*], C. WANG[a], M.Q. XUE[b], B.C. LIN[c], X. YE[a], W.N. LEI[a]
[a]*School of Mechanical Engineering, Jiangsu University of Technology, Changzhou 213001, Jiangsu Province, China*
[b]*Changzhou Vocational Institute of Light Industry, Changzhou, 213164, Jiangsu Province, China*
[c]*Jiangsu Key Laboratory for Solar Cell Materials and Technology, School of Materials Science and Engineering, Jiangsu Collaborative Innovation Center of Photovolatic Science and Engineering Changzhou University, Changzhou 213164, Jiangsu Province, China*

Ultrathin MoS_2 nanosheets at large scale were successfully synthesized by a facile hydrothermal solution reaction method, using hexaammonium heptamolybdate tetrahydrate ($(NH_4)_6Mo_7O_{24}$) and thiourea as the precursors. The final products were characterized by XRD, EDS, SEM and TEM. TEM and SEM images showed that the thickness of the obtained MoS_2 nanosheets was ~4 nm and the lateral size of the sheets was in the range of 200-400 nm. The influence of reaction temperature and time on the formation of MoS_2 nanosheets was discussed. A possible growth mechanism is proposed to explain the formation of MoS_2 nanosheets on the basis of observations of a time-dependent morphology evolution process.

(Received November 16, 2015; Accepted January 12, 2016)

Keywords: Hydrothermal synthesis; MoS_2; Nanosheets; Crystal growth; Nanocrystalline materials

1. Introduction

Since the discovery of graphene by Geim and coworkers [1] in 2004, ultrathin two-dimensional (2D) nanomaterials such as transition metal oxides, transition metal chalcogenides, and other 2D compounds have attracted intense attention due to the unusual properties associated with their ultrathin structure. [2,3] Ultrathin 2D nanostructures are expected to have the unique advantages of large exposed surface area and perfect interface, which make them a new class of emerging and promising materials for sensing, catalysis, electronic and energy storage applications, and so on. [4-9] Recently, considerable efforts have been devoted to developing different kinds of 2D nanomaterials. Among these 2D layered materials, MoS_2 has drawn wide attention because of its high chemical stability, low cost, and excellent electrocatalytic

*Corresponding author: zxhjstu@yahoo.com

performance[5,10-13].

To date, many methods have been employed to prepare ultrathin MoS_2 nanosheets. Coleman et al. [14] produced the two-dimensional nanosheets by liquid exfoliation of layered materials. Lee et al. [15] produced mono- and few-layer MoS_2 flakes by exfoliating the commercial MoS_2 powders in N-vinyl-2-pyrrolidone. Ramakrishna Matte et al. [16] employed three different methods to synthesize graphene-like MoS_2 and WS_2. Altavilla et al. [17] synthesized single- and few-layer nanosheets of MS_2 (M for Mo and W) by a wet chemical reaction. However, these approaches are frequently deficient in the yield of graphene-like production and the manufacturing processes of these approaches are complicated. Therefore, it is still a great challenge to develop simple, reliable and economical synthetic routes for preparing ultrathin MoS_2 nanosheets.

Herein, a facile hydrothermal approach was developed to synthesize ultrathin MoS_2 nanosheets. We also investigated the influence of the reaction time and temperature. On the basis of the evolution of the structure and the morphology with increasing the reaction time, a possible growth mechanism of ultrathin MoS_2 nanosheets structures is proposed.

2. Experimental

2.1. Synthesis

All of the chemical reagents were of analytic purity and used directly without further purification. The ultrathin MoS_2 nanosheets were synthesized by a one-step hydrothermal reaction using hexaammonium heptamolybdate tetrahydrate and thiourea as starting materials. In a typical synthesis, 1.24 g of hexaammonium heptamolybdate tetrahydrate and 2.28 g of thiourea were dissolved in 36ml deionized water under vigorous stirring for 30 min to form a homogeneous solution. The solution was then transferred into a 50ml Teflon-lined stainless steel autoclave and sealed tightly, heated at 220°C for 24 h and then naturally cooled down to room temperature. Black precipitates were collected by centrifugation and washed with distilled water and absolute ethanol for several times, and finally dried in vacuum at 60°C for 24 h.

2.2. Characterization

The X-ray diffraction (XRD) patterns were recorded using Japan Shimadzu LabX XRD-6000 X-ray diffractometer with Cu *Ka* radiation (λ = 0.1546 nm). The 2θ range used in the measurement was from 10° to 80° and the scanning rate was 5°min^{-1}. The morphologies of the as-synthesized products were examined by field-emission scanning electron microscopy (FESEM, JEOL, JSM-7001F) and transmission electron microscopy (TEM, JEOL, JEM-2100).

3. Results and discussion

Fig. 1a and b show the XRD diffraction patterns and EDS analysis of the as-prepared samples.As shown in Fig. 1a, all diffraction peaks in the XRD pattern can be readily ascribed to the pure hexagonal (P63/mmc space group) MoS_2 phase, with lattice constants a = 3.16 Å and c = 12.294 Å, which are in good agreement with the reported values (JCPDS card No. 37-1492). No

characteristic peaks from other impurities are observed in the XRD pattern, indicating that the sample was highly pure. Besides, the strong diffuse background and the weak (002) peaks were observed, indicating that the MoS_2 layers were of low stacking and highly disordered packing [18]. Energy-dispersive X-ray Spectrometer (EDS) was also used to examine the elemental composition of the samples. As shown in Fig. 1b, apart from the presence of element Mo and S, no other element was observed. Furthermore, the quantification of the peaks shows that the atom ratio between Mo and S is about 1:1.98, which is very close to the stoichiometric MoS_2.

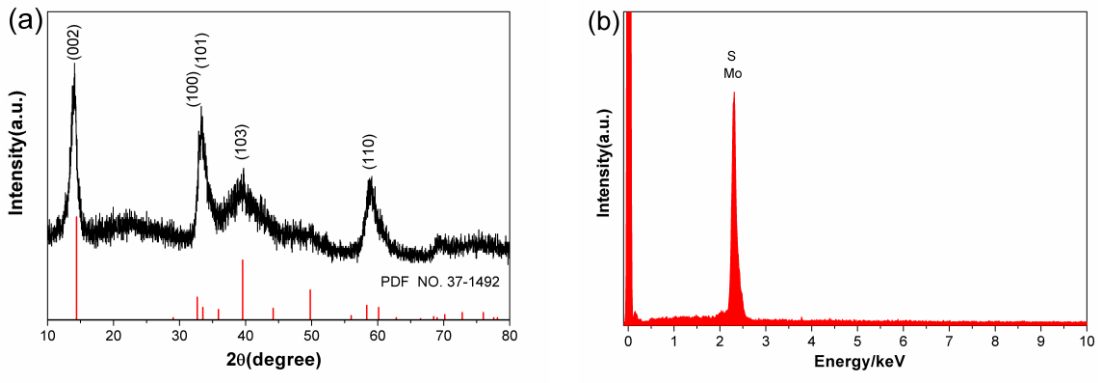

Fig. 1. (a) XRD pattern and (b) EDS of the as-prepared MoS_2 nanosheets

The morphology and size of the obtained products were further examined by SEM (Fig. 2a-b) and TEM (Fig. 2c-d). As shown in Fig. 2a, the samples were composed of many aggregated nanosheets. To reveal the clear view of the nanosheets, the high-magnification SEM image was recorded (Fig. 2b). It reveals that the obtained samples mainly comprised of the well-defined nanosheets, where the lateral size of the sheets is in the range of 200-400 nm. The yield of product with the foil-like thin sheets morphology was almost 100%.

In order to further reveal the morphology and microstructure of MoS_2 nanosheets, we carry out TEM measurements on the as-prepared samples. As shown in Figure 2(c), the low-magnification TEM image also verifies the ultrathin nanosheet morphology of the product and the result is coincident with SEM. The high-magnification TEM image, as shown in Fig. 2d, shows that the MoS_2 nanosheets are composed of 5-10 layers and the interlayer separation between the MoS_2 layers is about 0.64 nm, which is consistent with the (002) lattice plane of MoS_2.

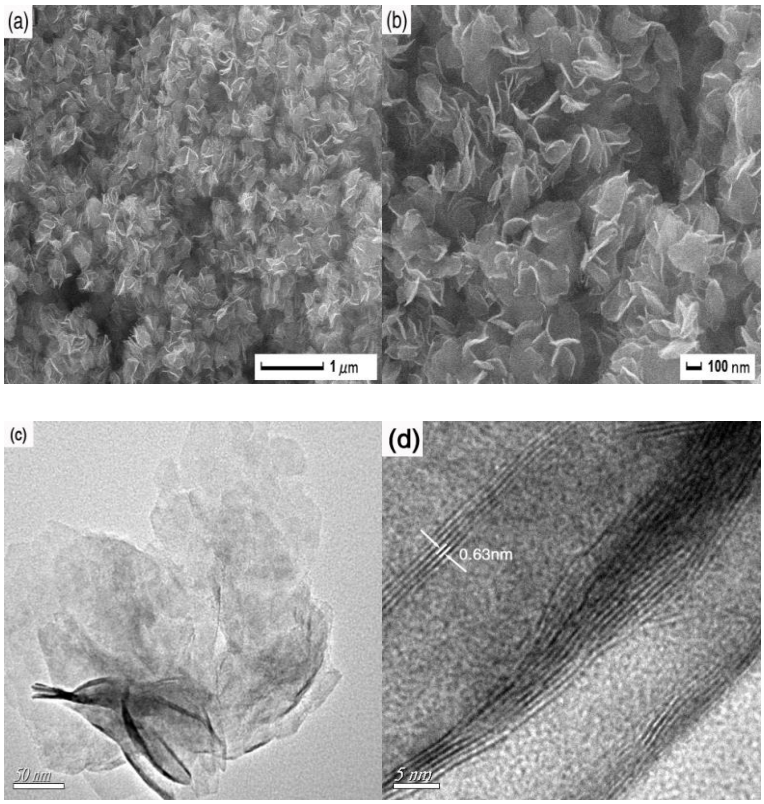

Fig. 2 SEM (a,b) and TEM (c,d) of the MoS_2 nanosheets.

To better understand the growth process of the ultrathin MoS_2 nanosheets, time-dependent experiments were carried out and the morphology evolution of intermediates involved in the formation process was investigated accordingly. As depicted in Fig. 3a, the products were composed of many aggregated nanosheets for aging period of 0.5 h. When the reaction time was increased to 2 h (Fig. 3b), the amount of microspheres was increasing owing to the initially formed nanosheets aggregate into spheres by self-assembly to minimize their surface energy. By further prolonging the reaction time to 6 h (Fig. 3c), the nanosheets disappeared and flowerlike microspheres assembled by nanosheets were obtained. As the reaction time was prolonged to 12 h (Fig. 3d), 3D flower-like MoS_2 spheres diminished gradually and dispersed into interconnected nanoplates. When the reaction time reached 24 h (Fig. 2a), only ultrathin nanosheets were observed. Similar nanosheet structure and size distribution were observed in samples obtained after 48 h of reaction (Figure 3e), suggesting that the morphological transformation and the nanosheet growth are mostly complete after 24 h of reaction. On the basis of these observations, the reaction time was the most important controlling factor.

Based on the above experimental results and the reported strategies in the synthesis of MoS_2 in literatures [19-21], we deduce that the formation of MoS_2 in this work go through a four-stage growth process, which involves a fast nucleation of amorphous primary particles; oriented aggregation of nanosheets; self-assembly of microsphere-structures and the formation of the ultrathin nanosheets by dispersion of the microsphere. To clearly demonstrate the evolution process of the MoS_2 nanosheets, a schematic illustration is given in Figure 4. Since the molar ratio of $(NH_4)_6Mo_7O_{24}$ to CSN_2H_4 is 1:30, more H_2S would be produced from the hydrolysis of thiourea and more MoS_2 nuclei would be formed at the first stage. Subsequently, MoS_2 nuclei would grow into nanoplates according to their crystal growth habit. When more nuclei were formed, this would

lead to the decrease of nutrient in solution for providing for the growth of MoS_2 nuclei, and further the decrease of nanoplate in size. Then the thinner MoS_2 nanoplates lead them to interwine and convolute to form flowerlike microspheres, driven by reducing surface energy. But the microspheres are not stable and finally they could be broken into discrete nanosheets after long-time reaction under high pressure in the autoclave. According to the previous studies[22–23], the following chemical reactions were suggested to be involved during the whole conversion process:

$$CSN_2H_4 + 2H_2O \rightarrow 2NH_3 + CO_2 + H_2S \quad (1)$$

$$(NH_4)_6Mo_7O_{24} \rightarrow 6NH_3 + 7MoO_3 + 3H_2O \quad (2)$$

$$MoO_3 + 3H_2S + H_2O \rightarrow MoO_2 + SO_4^{2-} + 2H^+ \quad (3)$$

$$MoO_2 + 2H_2S \rightarrow MoS_2 + 2H_2O \quad (4)$$

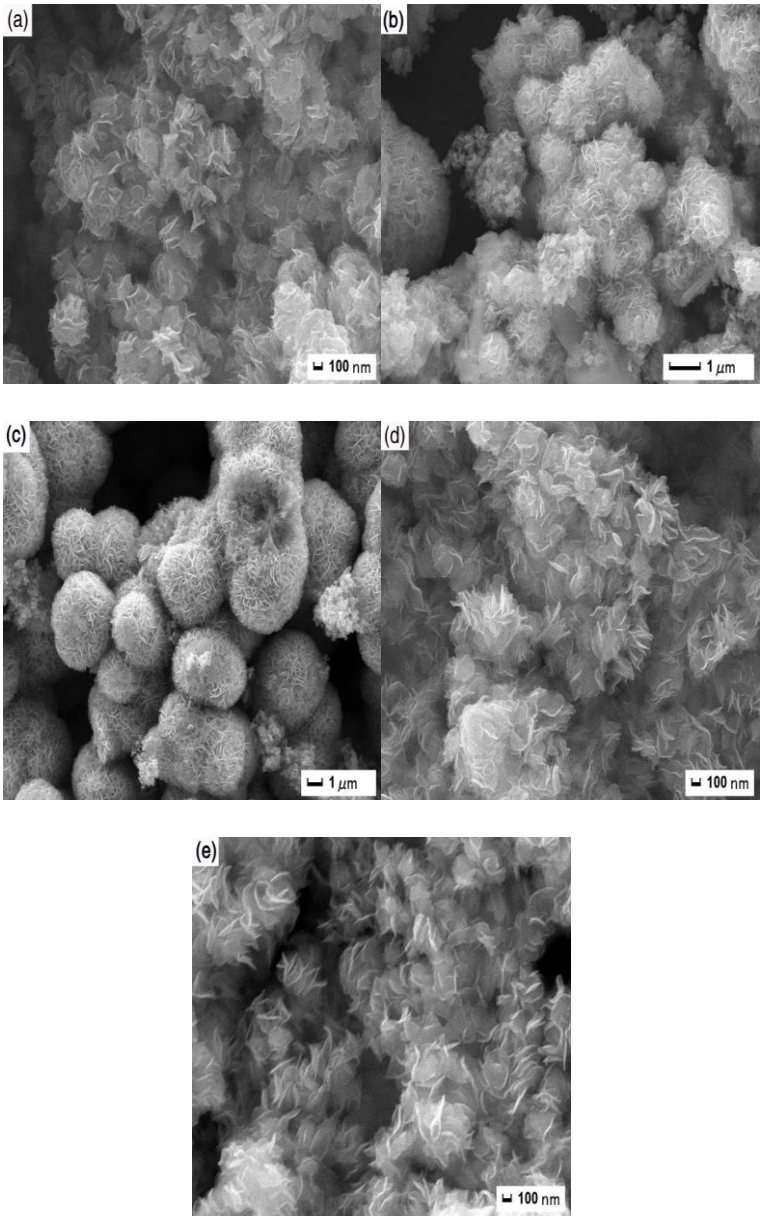

Fig. 3 SEM images of the products obtained at reaction times of (a) 30 min, (b)2 h, (c) 6 h, (d) 12h and (e) 48 h.

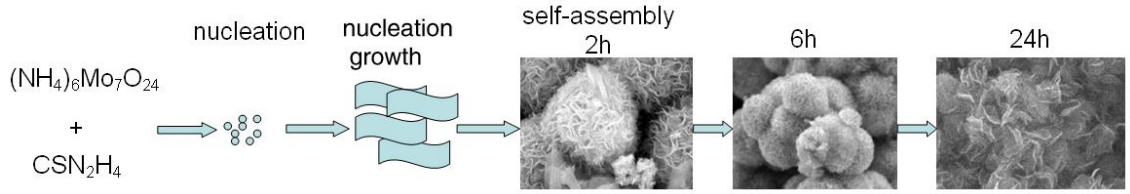

Fig. 4 Schematic illustration of the morphological evolution process of the ultrathin MoS_2 nanosheets.

It was also found that the reaction temperature is very important for the synthesis of the ultrathin MoS_2 nanosheets. To study the effect of the hydrothermal treatment temperature on the morphologies of the obtained materials, MoS_2 nanosheets were prepared at different temperature for 24 h. The XRD results and SEM images of the as-prepared samples were shown in Fig. 5a-d. Fig. 5a shows typical XRD patterns of the samples obtained at 160 °C, 180 °C , 200°C and 220°C. When the reaction temperature is at a lower temperature (160 °C and 180 °C), only two lower intensities peaks located at the (100) and (110) positions of MoS_2 can be detected, which implies that only poor crystal were produced. With the increasing of the reaction temperature up to 200°C, a small peak with 2θ of 14.4° corresponding to diffraction from the (002) plane of MoS_2 appeared, revealing the stacking of the single layers of MoS_2 take place. When the reaction temperature rises to 220°C, the intensity of the detected diffraction increased obviously. From the XRD patterns, it could be observed that reaction temperature had some effects on the crystal growth of MoS_2 and the crystallinity of the products could be greatly improved with the increasing reaction temperature.

The SEM images of the corresponding samples obtained at 160 °C, 180 °C and 200 °C are shown in Fig. 5b, 5c and 5d, respectively. From Fig. 5b and 5c, it could be observed that the sample obtained at 160 ℃ and 180 °C were mainly composed of aggregated particles, which showed a "rag-like" morphology just like the poorly crystalline MoS_2 reported by Peng et al. [24]. When the reaction temperature is raised to 200 °C, the crystal morphology becomes clearer and shows a sheet structure(Fig. 5d). The above experimental results demonstrate that the morphologies of the MoS_2 structures are sensitive to the hydrothermal temperature.

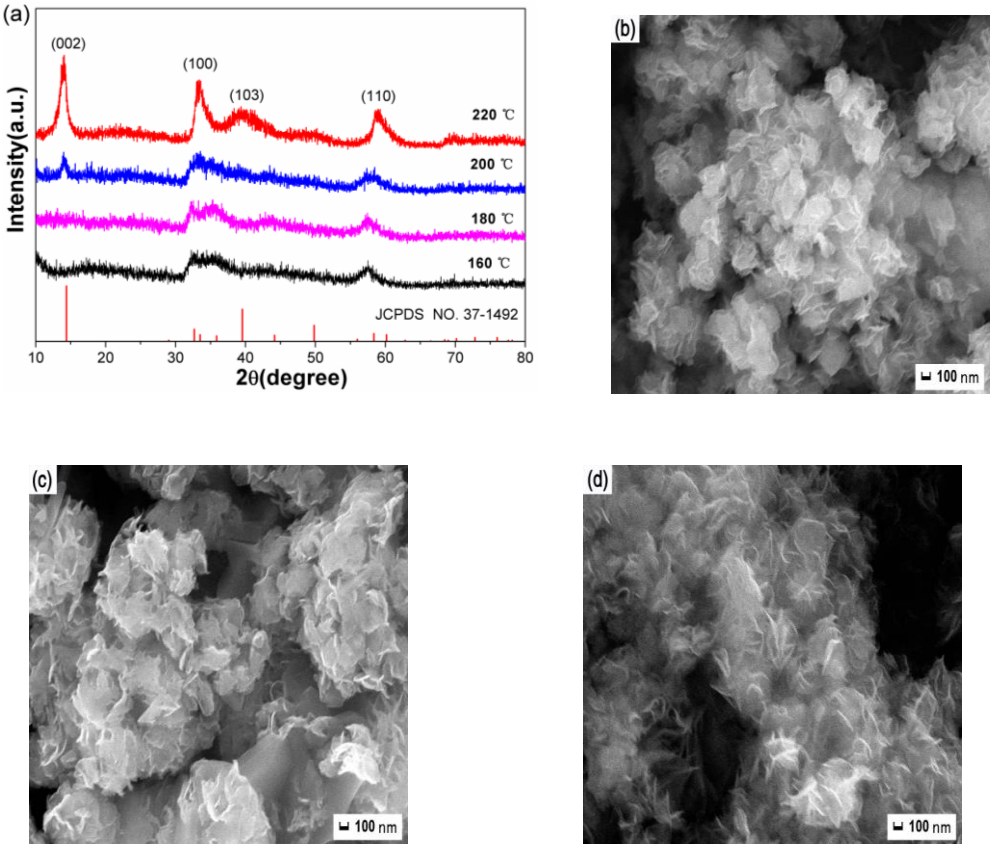

Fig. 5 (a) XRD patterns of the samples obtained at different temperatures. (b) - (d) the SEM images of the MoS_2 nanosheets obtained at 160 °C, 180 °C and 200 °C for 24 h

4. Conclusion

In this study, a facile and scalable approach for fabricating ultrathin MoS_2 nanosheets was presented by the reaction of hexaammonium heptamolybdate tetrahydrate and thiourea at temperature of 220 °C for 24h. MoS_2 nanosheets with thickness ~4 nm and lateral size of about 200-400 nm were successfully synthesized. The experimental results suggest that the reaction time and temperature plays a crucial role in the formation of ultrathin MoS_2 nanosheets. Moreover, a possible growth mechanism was proposed to explain the formation of the ultrathin MoS_2 nanosheets. Considering the simple synthetic process, it is believed that the approach presented here can be extended to synthesize other metal sulfides nanomaterial.

Acknowledgements

This work was financially supported by the Natural Science Foundation of the Jiangsu Higher Education Institutions of China (14KJB460012), the Changzhou Sci&Tech Program(CJ20159048), the research fund of Jiangsu Province Cultivation base for State Key Laboratory of Photovoltaic Science and Technology(SKLPSTKF201508), the Natural Science

Foundation of Jiangsu University of Technology (KYY14003), and Innovation Training Programs for Undergraduates of Jiangsu Province (201511463008Z)

References

[1] K. S. Novoselov, A. K. Geim, S. V. Morozov, D. Jiang, Y. Zhang, S. A. Dubonos, et al., Science **306**, 666(2004).
[2] M. S. Xu, T. Liang, M. M. Shi, H. Z. Chen, Chem. Rev. **113**, 3766(2013).
[3] F. Léonard, A. A. Talin, Nat. Nanotechnol. **6**, 773(2011).
[4] B. Cho, M. G. Hahm, M. Choi, J. Yoon, A. R. Kim, Y. J. Lee, et al., Scientific reports **5**,8052(2015).
[5] Q. H. Wang, K. Kalantar-Zadeh, A. Kis, Nat. Nanotechnol. **7**,699(2012).
[6] Y. Yan, B. Y. Xia, X. Ge, Z. Liu, J. Y. Wang, X. Wang, ACS Appl. Mater. Inter. **5**,12794(2013).
[7] Q. Zhang, H. X. Liu, H. L. Li, Y. Liu, H. Y. Zhang, T. Li, Appl. Surf. Sci. **328**,525(2015).
[8] E. Yoo , J. Kim , E. Hosono , et al. , NanoLett. **8**, 2277(2008) ;
[9] R. B. Jacobs-Gedrim , M. Shanmugam ,N. Jain , et al., ACS Nano **8** , 514 (2014);
[10] D. Merki, S. Fierro, H. Vrubel and X. L. Hu, Chem. Sci. **2**, 1262(2011).
[11] D. Merki, H. Vrubel, L. Rovelli, S. Fierro, X. L. Hu, Chem. Sci. **3**, 2515(2012).
[12] J. F. Xie, H. Zhang, S. Li, R. X. Wang, X. Sun, M. Zhou, etal., Adv. Mater. **25**, 5807(2013).
[13] N. Liu, L. C. Yang, S. Wang, Z.W. Zhong, S.N. He, X.Y. Yang, Q.S. Gao, J. Power Sources **275**, 588(2015)
[14] J. N. Coleman, M. Lotya, A. O′Neill, S. D. Bergin, P. J. King, Science **331**,568(2011).
[15] K. Lee, H.Y. Kim, M. Lotya, J. N. Coleman, G.T. Kim, G.S. Duesberg, Adv. Mater. **23**, 4178 (2011).
[16] H.S.S. Ramakrishna Matte, A. Gomathi, A. K. Manna, D. J. Late, R. Datta, S. K. Pati, et al., Angew. Chem. **122**, 4153(2010).
[17] C. Altavilla, M. Sarno, P. Ciambelli, Chem. Mater. **23**, 3879(2011).
[18] Z.Z. Wu, D.Z. Wang, A.K. Sun, Mater. Lett. **63**, 2591(2009).
[19] G.G. Tang, J. R. Sun, W. Chen, K. Q. Wu, X. R. Ji, S. S. Liu, Mater. Lett. **86**, 9 (2012).
[20] Ma L, Xu L M, Xu X Y, Luo Y L, Chen W X. Mater. Lett. **63**, 2022 (2009).
[21] X.H. Zhang, X.H. Huang, M.Q. Xue, X.Ye, W.N. Lei, H. Tang, C.S. Li, Mater. Lett. **148**, 67(2015).
[22] Feng C, Ma J, Li H, Zeng R, Guo Z P, Liu H K. Mater. Res. Bull. **44**, 1811 (2009).
[23] H. A. Therese, N. Zink, U. Kolb, W. Tremel, Solid State Sci. **8**, 1133(2006).
[24] Y. Peng, Z. Meng, C. Zhong, J. Liu, Z. Yang, Y.T. Qian, Mater. Chem. Phys. **73**, 327 (2002).